Electronic Supplementary Material (ESI) for Lab on a Chip

Thermal Migration of Molecular Lipid Films as Contactless Fabrication Strategy for Lipid Nanotube Networks

Supplementary Information

SI 1. Materials and Methods

Vesicle preparation:

Five different lipid recipes have been used. The ratio (wt %) of alternating lipid types/fluorophores are summarized in Table SI 1. below.

Table SI 1. Lipid compositions.

Lipid abbreviation	PC	PI	PA	PE	Other	Texas-Red DHPE	ATTO-488	ATTO-655	Thermomigr.	Figure
PC-PI-594	69	30	-	-	-	1	-	-	+	Figure 1
PC-PI-488	69	30	-	-	-	-	1	-	+	Not shown
PC-PI-655	69	30	-	-	-	-	-	1	+	Figure 2
PC-PI-PE	20	30	-	49	-	1	-	-	-	Not shown
Soy-Bean	45	18	7	22	7	-	-	1	-	Not shown

Soy L-α Phosphatidyl choline (PC), Soy L-α Phosphatidyl inositol (PI), Soy L-α Phosphatidyl etanolamine (PE) and Soy Bean Polar Lipid Extract (SPE) were obtained from Avanti Polar Lipids (Alabama, USA). 7% of the content of SPE is unspecified by the manufacturer. Texas Red 1,2-dihexadecanoyl-sn-glycero-3-phosphoethanolamine (DHPE) was obtained from Life Technologies (Sweden) and both ATTO dyes from ATTO-Tech (Germany).

For each recipe, 10 mg/ml lipid-dye stock solution was prepared[1]. 3 µl of each suspension were dehydrated for 15 min on a cover slip in an evacuated desiccator. The dry lipid films were subsequently rehydrated with 1 ml of 10 mM HEPES buffer (contains only 10 mM HEPES and 100 mM NaCl, pH 7.8 adjusted with NaOH, Sigma) for 10 min to allow formation of multilamellar vesicles (MLVs). MLV samples were transferred into an observation chamber with an Aluminum coated cover slip at the bottom, containing 5 ml of 10 mM HEPES buffer with 4 mM $CaCl_2$. After MLVs spread, the buffer

solution containing 10 mM HEPES, 100 mM NaCl, 10 mM BAPTA (pH=7.8 adjusted with NaOH) was slowly injected into the observation chamber via an automatic pipette. By the same means the ambient buffer containing 4 mM Ca^{2+} was removed. Deionised water was obtained from a Milli-Q system (Millipore).

Surface fabrication:

All steps of surface fabrication were performed in the clean room facility MC2, at Chalmers University of Technology (class 3-6 according to ISO 14644-1).

Plain Surfaces: Glass cover slips (Menzel Gläser) were pre-cleaned by sonication for 5 minutes in the presence of Microposit remover 1165 (Shipley), washed with water and blow-dried. For all depositions, a MS 150 Sputter system (FHR Anlagenbau GmbH) was used. An aluminum film was deposited onto the cleaned glass substrate by direct current (DC) sputtering to a final film thickness of 10 nm. The Al surfaces were subsequently oxygen plasma treated for 5 minutes in a Plasma etch BatchTop PE/RIE m/95 (Plasma Therm; FL, USA). Al_2O_3 and SiO_2 films were deposited by reactive (RF) sputtering on a pre-cleaned surface to a final film thickness of 10 and 84 nm, respectively.

SU-8 pillars: The glass coverslips were thoroughly cleaned in a megasonic water bath for 10 minutes, rinsed with MQ water, blow-dried, and treated with oxygen plasma for 2 minutes (10 sccm oxygen, 250 mbar, 50 W, BatchTop PE/RIE m/95 (Plasma Therm; FL, USA). 2 nm of Ti film were deposited with DC sputtering prior to SU-8 coating. SU-8 2002 photoresist (Microchem) was spin-coated onto coverslips to a thickness of ~ 3 µm, and subsequently soft baked for 2 minutes at 95°C. This cycle was applied 3 times until the final thickness (~ 4 µm) was reached. The coverslips were exposed to UV light (400 nm) in a Süss MicroTec MA6 mask aligner for 40 seconds. The exposed substrates were post baked for 1 min at 65°C, followed by 2-3 min at 95°C. The cover slips were submerged into SU-8 developer (mr-Dev 600, Micro Resist Technology) for 5 minutes. In the final step, the coverslips were rinsed with isopropanol and water, and blow-dried with nitrogen. The dark-field photomask for the SU-8 process was prepared using a JEOL JBX-9300FS electron beam lithography system. A UV-5/0.6 resist (Shipley Co.) coated Cr/soda-lime mask was exposed, developed and etched using a common process for micrometer resolution[2]. Pattern files were prepared on the Auto CAD 2007 (Autodesk Inc.) platform. On the structured surfaces, Al was deposited and subsequently etched as described above for the plain substrates. The final height of the SU-8 pillars has been determined using a Dektak D150 Surface Profiler (Veeco).

SPM imaging:

Scanning probe microscopy (SPM) was performed in tapping mode, using a Veeco Dimension ICON with a high resolution probe (Hi'RES-C - Cr/Au coated Si, 1 nm spike radius, Micromasch, Estonia) for imaging of the aluminum and silicon oxide surfaces.

SEM imaging:

Scanning electron micrographs were obtained using a Zeiss Supra 60 VP (IXRF EDX), using the SE2 and In-lens secondary electron detectors.

Microscopy imaging:

An inverted microscope (Leica DM IRB, Wetzlar, Germany), equipped with a Leica PL Fluotar 63x objective, and a DFK 23GP031 (The Imagingsource, Germany) GigE CMOS Color Camera was used for

imaging. Texas Red-DHPE was excited at 532 nm by a solid state laser (MGL-III-532, Changchun New Industries, Changchun, China). ATTO-488 and ATTO-655 were excited at 488 nm and at 644 nm, respectively, by diode lasers (Figure SI 2).

Data analysis:

Laser fluorescence micrographs were sharpened and the noise was removed with the NIH Image-J software package. Schematic drawings and image overlays were created with Adobe Illustrator CS4 (Adobe Systems, USA). Vesicle motion (**Figure 1n**) was analyzed from a high speed video using custom made image analysis script in Mathworks MATLAB. The experimental distance-time relation was fitted with a 3rd order polynomial.

SI 2. Infrared Laser Setup

Laser Assembly: The IR-B laser was assembled and tuned in-house. A 1470nm 3.8W diode laser (Seminex Inc., Peabody, MA, USA) was coupled to a 105 um (core diameter) multi-mode optical fiber with a NA of 0.22. The diode laser is powered by a 3V, 10A laser diode driver (Lumina Power Inc., Bradford, MA, USA) and controlled by an in-house built control unit.

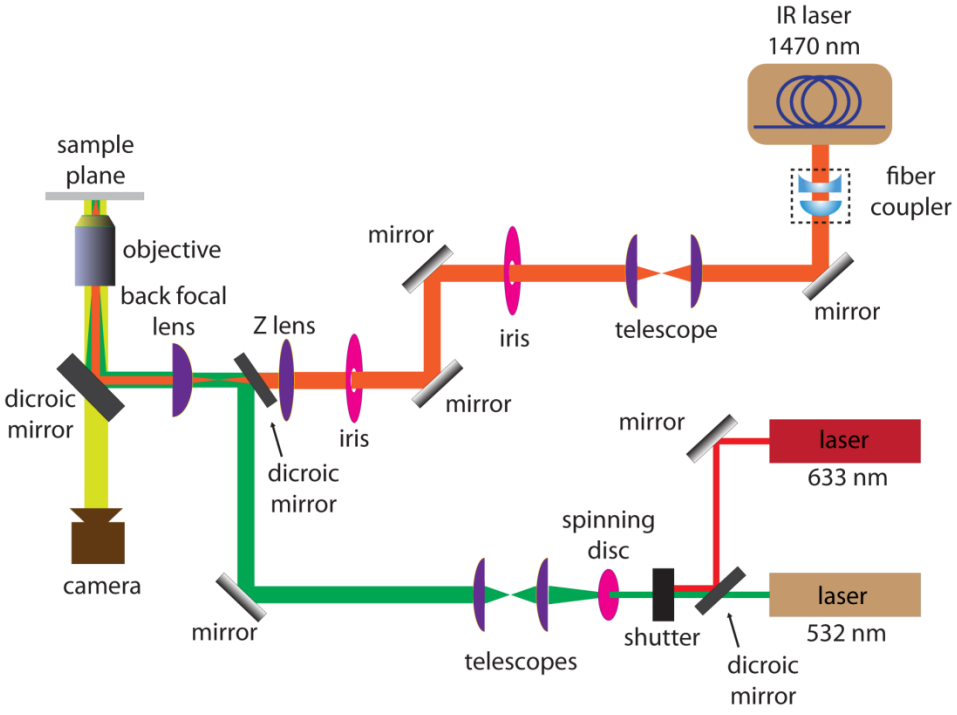

Figure SI 2. IR Laser setup. *Point heating was implemented through the use of an objective focused IR-B laser, directed to the microscope as per the schematic outline. Briefly, the output of the optical fiber, coupled to a 1470 nm diode laser, was collimated using a 0.25NA fiber collimator (Thorlabs). This beam was expanded and artifacts were removed with an iris. To collimate the light into the objective an additional Z-lens was needed to compensate for the back focal lens used for the epi-fluorescent illumination beam. To control the beam spot size in the sample plane, an iris was used before the z-lens,*

to decrease the beam diameter, lowering the effective NA of the objective, increasing the spot size. The 63x 1.32 NA objective, would yield a spot size of approximately 0.56 um using Abbe's equations. Due to beam irregularities and polarization, at its smallest size, the effective exposed spot would be <1um. By tuning the iris, to change only the IR-B beam objective NA, lowering it to approximately 1.0, resulting in an effective spot size of 2-3 µm.

SI 3. Surface Characterization

Surface properties of plasma treated Al surfaces:

We have performed scanning probe microscopy (SPM) (Veeco Dimension ICON SPM) in tapping mode using the Hi'RES-C (Micromasch, Estonia) high resolution probe on plasma treated substrates.

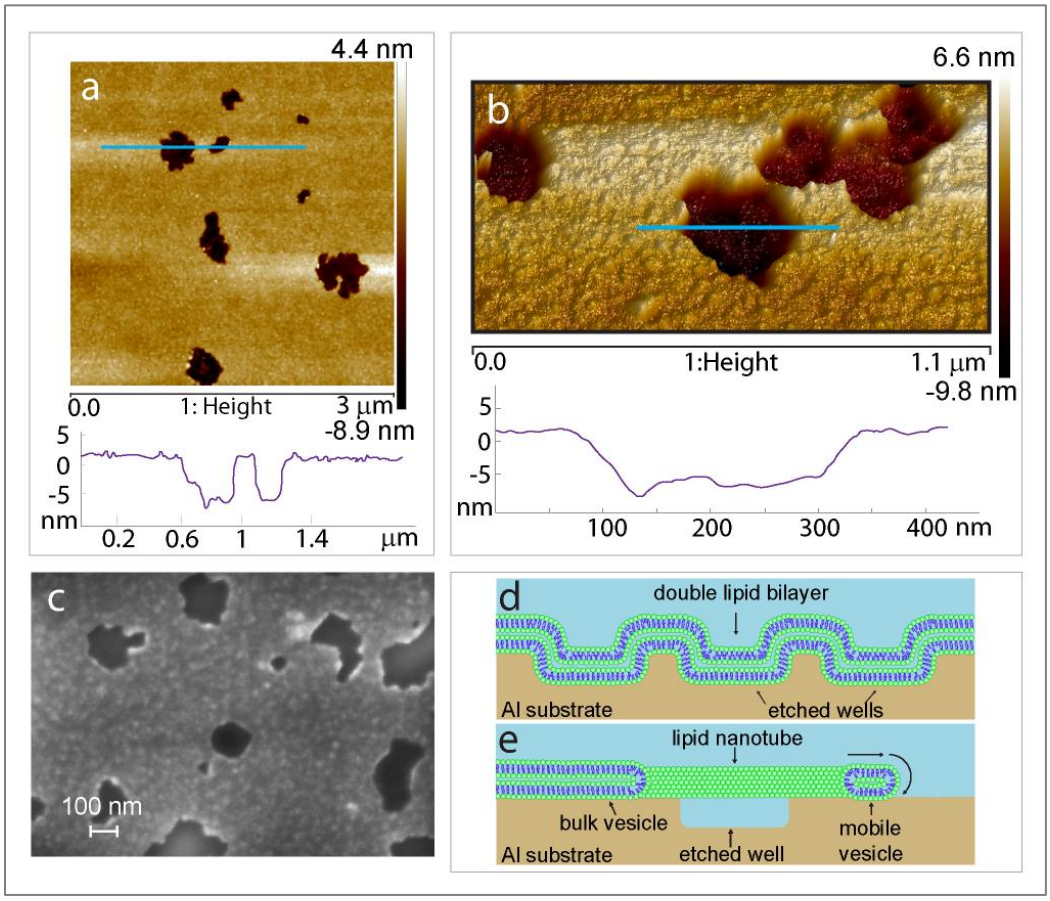

Figure SI 3.1 Surface characterization of thermotactic surface. ***(a)*** *2-dimensional (2D) AFM scan of a selected region from a plasma etched Al surface. The roughness profile is measured across the blue line.* ***(b)*** *3-dimensional (3D) detailed AFM scan of a region from an etched Al surface on a glass substrate. The roughness profile is measured across the blue line. The depth of the etched regions is around 6-8 nm.* ***(c)*** *Scanning electron micrograph (SEM) of a plasma etched Al surface on glass substrate. (a-c) reveal the wells with irregular morphology which are formed by O_2 plasma treatment.* ***(d)*** *Schematic of the cross sectional profile of the double bilayer lipid membrane on the plasma etched Al surface. The membrane*

follows the surface structures during spreading or migration. ***(e)*** *Schematic of the cross sectional profile of a suspended nanotube across the well during the migration of a mobile vesicle.*

Substrate Topography of Al_2O_3 and SiO_2 surfaces:

For comparison of the surface roughness of the different substrates we have performed scanning probe microscopy (SPM) (Veeco Dimension ICON SPM) in tapping mode on sputtered Al_2O_3 and SiO_2 substrates in addition to the etched Aluminum (Figure SI 3.1) for comparison.

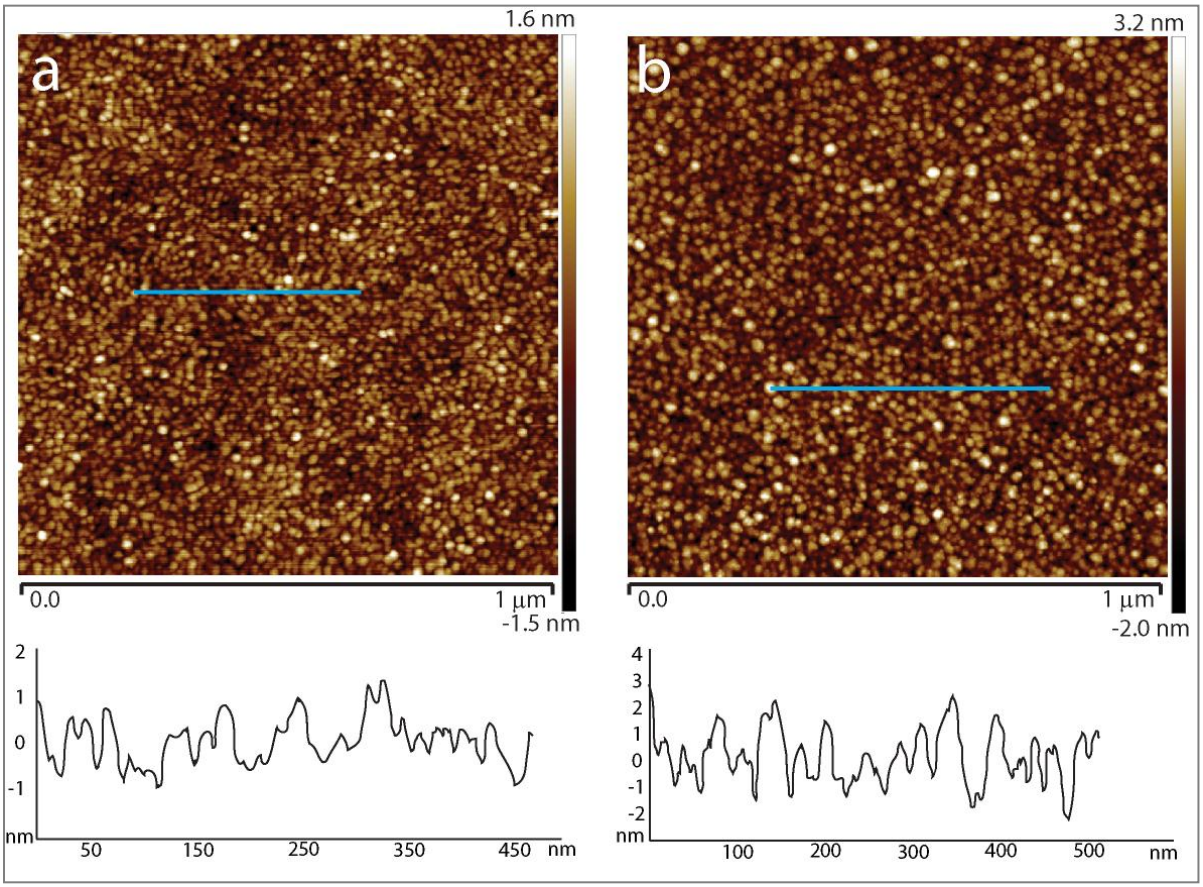

Figure SI 3.2. Substrate topography of (a) Al_2O_3 and (b) SiO_2. *The insets show the roughness along the blue lines of each surface. The SiO_2 grains appear to be bigger than Al_2O_3 grains, and the latter has a slightly lower roughness. The images have been flattened using the NanoScope Analysis Software 1.20 (Veeco).*

Surface Zeta Potential:

Zeta potential measurements of substrates were performed by Ebatco (MN, USA). The values are based on electrophoretic light scattering conducted using a Delsa NanoC instrument (Ebatco, USA) in a flat surface cell at room temperature. 100 mM standard NaCl solution was used to measure the cell constants. The zeta potential values of sputtered SiO_2, oxidized Al and sputtered Al_2O_3 were measured to be -31.87 mV, -1.48 and 4.45, respectively, as depicted in Figure SI 3.3 .

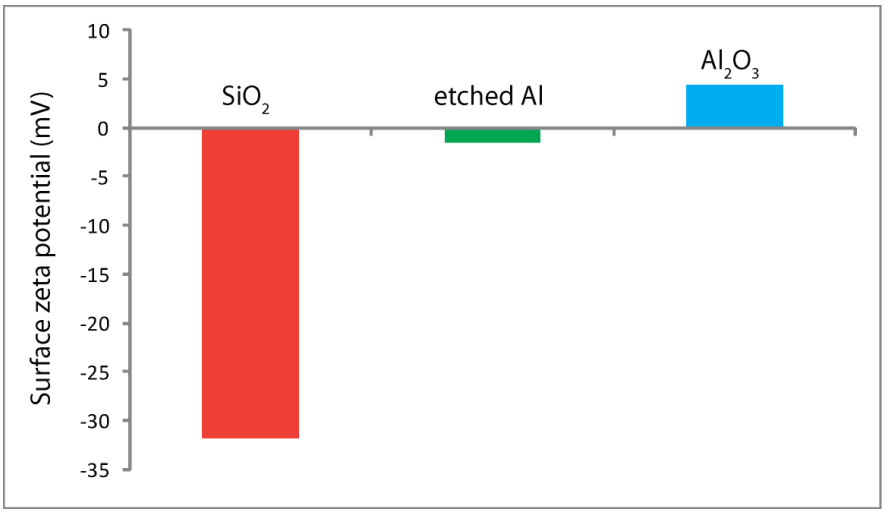

Figure SI 3.3. Zeta Potential of solid surfaces. *The graph shows the zeta potentials for the 3 substrates used in the study: -31.87 mV for SiO_2, -1.48 for plasma treated Al and 4.45 for Al_2O_3.*

SI 4. Temperature Measurements

To estimate the local temperature in the aqueous solution reached by the IR laser heating, we performed an experiment using a lower critical solution temperature (LCST) polymer: PNIPAm (Poly *N*-isopropyl acrylamide) (Sigma-Aldrich). The LCST (coil to globule transition) of PNIPAm is ~ 32 °C[3]. Above this critical temperature PNIPAm switches from a swollen hydrated phase to a collapsed dehydrated phase.

We initiated the experiment by placing a drop of aqueous PNIPAm solution onto the substrate at room temperature (20 °C). The temperature of the solution was established with a micro-thermocouple (Omega Engineering, UK).

We then exposed the polymer solution with the beam of the IR laser, using the exact same intensity as we apply to manipulate the flat vesicles. During this exposure, PNIPAm does not exhibit any clouding. This means that the temperature which is reached in the vicinity of the substrate does not reach 32 °C. Therefore the temperature interval where the thermotaxis behavior of flat lipid vesicles is observed is between 20 - 32 °C. When we increased the IR laser intensity above the designated value, PNIPAm eventually changed to a shrunken dehydrated state, and formed a spot of ~20 µm size. This state of the polymer was used to determine the temperature gradient as discussed below.

Characterization of laser microheating:

The microscope was focused on the surface and gel images were recorded at different laser powers P. In each case the optical power was also measured at the output of the laser, using a laser power meter Coherent Field Max II-TO, equipped with Coherent Power Max PM10 thermopile sensor (Coherent Inc. USA). At each point, the system was given a few second to reach a stationary temperature distribution. In the calculations we assume that the temperature profile $T(r,P) - T_0 \propto P$. The room temperature $T_0 = 20\ ℃$. From each image, the radius r_P was extracted, where the temperature is above T_P (Figure SI 4). These data points form a relation $P_P(r)$, describing the power needed for certain spot size r. Then, the temperature profile $T(r,P_e)$, for the actual experimental power P_e can be constructed as

$$T(r, P_e) = T_0 + \frac{P_e}{P_P(r)}(T_P - T_0)$$

The measured temperature profile was fitted with a power function $T(r) = T_0 + a \cdot (r/1\ \mu m)^{\ b}$, which yielded for the power used in the measured region

$$T(r) = 20\ ℃ + 22.2\ ℃ \cdot \left(\frac{r}{1\ \mu m}\right)^{-0.827}$$

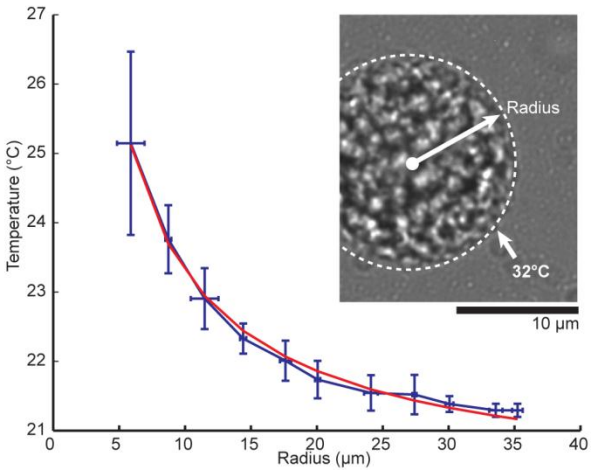

Figure SI 4. Laser microheating characterization. *The figure shows the measured temperature profile (blue) and the fit (red). The inset shows the concept of temperature measurement, where the region with a temperature above 32°C, was estimated from a brightfield microscopy image. Uncertainties are given at the 95% confidence level.*

The fit can be used for analytical calculations as well as to find a gradient, which would be

$$\nabla T(r) = -18\ \frac{℃}{\mu m}\left(\frac{r}{1\ \mu m}\right)^{-1.827}$$

This is close to gradients produced by a point heater $\nabla T(r) \propto r^{-2}$. Slight deviations are most likely due to more broad and complex heating profile of the optical heater, where both surface absorption (in metal) and strong absorption in water contribute, along with inhomogeneous spatial illumination due to a steep spread of light around the high NA focus. In case of a point heater this result would correspond to heating power about 0.1-0.2 mW.

Analysis of the frames of Figure 1 j-m reveals that in the thermomigration experiments, the beginning of the mobile vesicle is at a distance of 16.2 (51) µm from the heat source center, and its end at 32.0 (88) µm (statistical variance at one σ). This allows estimating the temperature difference over the mobile vesicle as ~**1°C** (Fig. SI 4).

SI 5. Additional Thermomigration Experiments

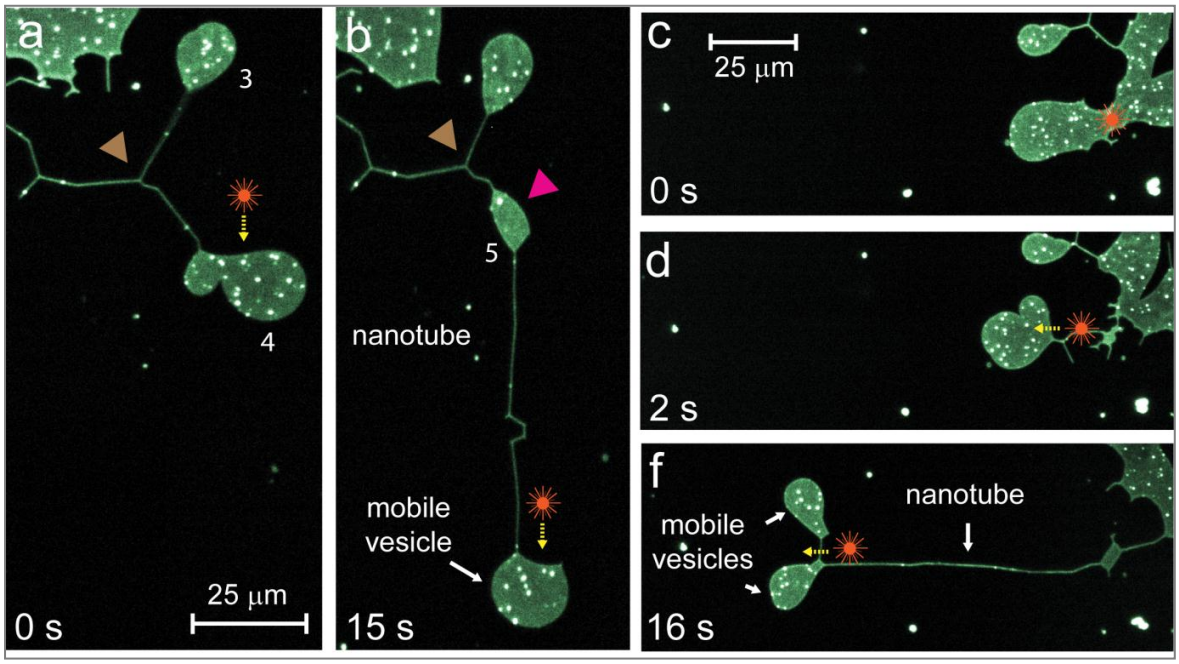

Figure SI 5. Additional images showing thermomigration of vesicles (supplementary to Figure 1 of the main article). ***(a,b)*** *Laser fluorescence microscopy image, showing additional mobile vesicles formed by lR-laser fragmentation in the experiment depicted in Figure 1 of the main article. The vesicles are consequently numbered as #3, #4 and #5. The brown arrow heads show a lipid nanotube Y-junction, similar to the ones in Figure 1 of the main article, the pink arrow head points to the origin of vesicle #5.* ***(c)*** *Image of a separating vesicle from a different bulk membrane patch.* ***(d-f)*** *Thermomigration of the mobile vesicle released in* ***(c)****. A lipid nanotube is formed, and the vesicle is divided into two smaller mobile vesicles*.

SI 6. Videos

Videos recordings of the experiment shown in figure 1, figure 2, and figure SI 5 are provided as additional content.

References

1. *M. Karlsson, K. Nolkrantz, M. J. Davidson, A. Stromberg, F. Ryttsen, B. Akerman and O. Orwar, Analytical Chemistry, 2000, **72**, 5857-5862.*
2. *J. Zhang, K. L. Tan, G. D. Hong, L. J. Yang and H. Q. Gong, Journal of Micromechanics and Microengineering, 2001, **11**, 20-26.*
3. *A. Burmistrova, R. Steitz and R. Von Klitzing, ChemPhysChem, 2010, **11**, 3571-3579.*